

Comparison of gluon flux-tube distributions for quark-diquark and quark-antiquark hadrons

F. Bissey and A. I. Signal

*Institute of Fundamental Sciences, Massey University,
Private Bag 11 222, Palmerston North, New Zealand*

D. B. Leinweber

*Centre for the Subatomic Structure of Matter and
School of Chemistry and Physics, University of Adelaide, SA 5005, Australia*

The distribution of gluon fields in hadrons is of fundamental interest in QCD. Using lattice QCD we have observed the formation of gluon flux tubes within three quark (baryon) and quark plus antiquark (meson) systems for a wide variety of spatial distributions of the color sources. In particular we have investigated three quark configurations where two of the quarks are close together and the third quark is some distance away, which approximates a quark plus diquark string. We find that the string tension of the quark-diquark string is the same as that of the quark-antiquark string on the same lattice. We also compare the longitudinal and transverse profiles of the gluon flux tubes for both sets of strings, and find them to be of similar radii and to have similar vacuum suppression.

PACS numbers: 12.38.Gc, 12.38.Aw, 14.70.Dj

I. INTRODUCTION

There has recently been a renewal of interest in the properties of diquarks in hadronic systems, as they may play an important role in the existence of exotic states, such as the Θ^+ , or in explaining the scarcity of such exotics [1]. While string-type models consisting of a quark plus a diquark have been studied using various analytic techniques (see [2] for a review), there have only been a few studies of this type of system on the lattice. These studies have investigated the mass of diquarks [3, 4, 5, 6, 7], and, more recently, the nature of diquark correlations [8]. Recently we investigated the formation of flux tubes in static baryon systems on the lattice using a high statistics approach which enabled us to observe correlations between the vacuum action density and the quark positions in a gauge independent manner [11]. In that work the three quarks were positioned approximately equidistant, and a Y-shaped flux-tube was observed to form at large inter-quark distances. In this work we extend our study of three quark systems to the case where two of the quarks are close together and the third is some distance away.

In QCD, two quarks close together, a diquark, can transform either according to the conjugate representation ($\bar{3}$) or the sextet (6) representation of $SU(3)$. The color hyperfine interaction then leads to attraction in the spin singlet, scalar diquark channel, while the spin triplet, axial vector diquark is disfavoured. Hence low-lying diquarks should have positive parity and belong to the color $\bar{3}$ representation, and so have many properties similar to an antiquark. In lattice QCD this should lead to the formation of quark-diquark flux tubes with similar physical characteristics to those of quark-antiquark flux tubes. In particular we would expect the long range

linear part of the quark-diquark potential to have the same slope as that of the quark-antiquark potential, corresponding to the flux tubes having the same energy density, and we would expect the flux tubes to have similar transverse size. In this work we investigate whether these similarities do indeed hold.

II. FLUX TUBES ON THE LATTICE

In order to study flux-tubes on the lattice, we begin with the standard approach of connecting static quark (and antiquark) propagators with spatial-link paths in a gauge invariant manner. We use APE-smearing spatial-link paths to propagate the quarks from a common origin to their spatial positions as illustrated in Fig. 1. In earlier work we saw that after approximately 30 APE smearing steps we had obtained optimal overlap with the ground state. The static quark propagators are constructed from time directed link products at fixed spatial coordinate, $\prod_i U_i(\vec{x}, t_i)$, using the untouched ‘thin’ links of the gauge configuration. In principle, the ground state is isolated after sufficient time evolution. Finally smeared-link spatial paths propagate the quarks back to the common spatial origin.

The three-quark Wilson loop is thus defined as:

$$W_{3Q} = \frac{1}{3!} \varepsilon^{abc} \varepsilon^{a'b'c'} U_1^{aa'} U_2^{bb'} U_3^{cc'}, \quad (1)$$

where U_j is a staple made of path-ordered link variables

$$U_j \equiv P \exp \left(ig \int_{\Gamma_j} dx_\mu A^\mu(x) \right), \quad (2)$$

and Γ_j is the path along a given staple as shown in Fig. 1. In contrast the quark-antiquark Wilson loop is given by

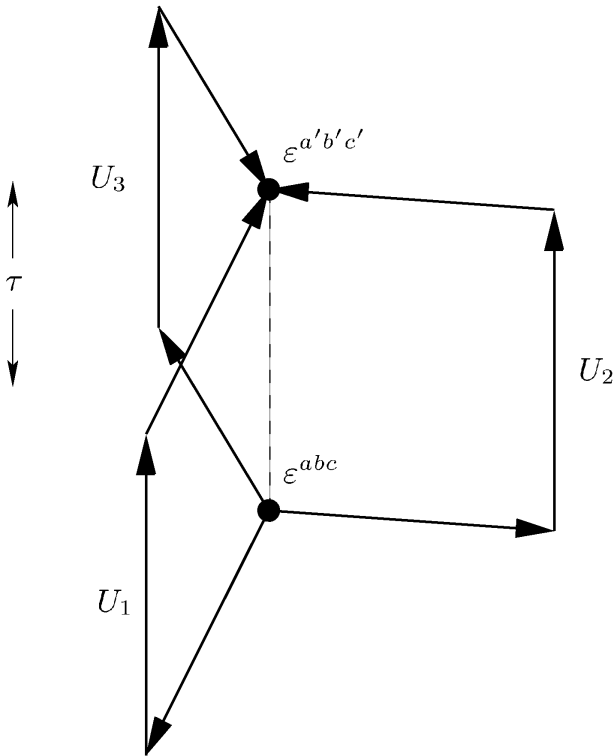


FIG. 1: Gauge-link paths or “staples,” U_1 , U_2 and U_3 , forming a three-quark Wilson loop with the quarks located at \vec{r}_1 , \vec{r}_2 and \vec{r}_3 . ε^{abc} and $\varepsilon^{a'b'c'}$ denote colour anti-symmetrisation at the source and sink respectively, while τ indicates evolution of the three-quark system in Euclidean time.

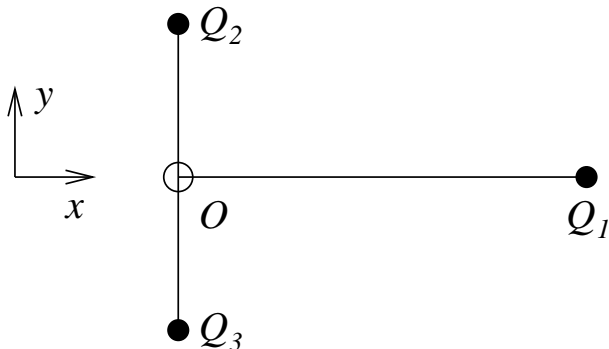


FIG. 2: Projection of the T-shape path on the x - y plane.

the product of two staples

$$W_{Q\bar{Q}} = \delta^{ab}\delta^{a'b'} U_1^{aa'} \left(U_2^{bb'} \right)^\dagger. \quad (3)$$

The three-quark configurations we use to approximate a quark-diquark string are T-shapes, with the origin at the junction of the T. Two quarks are positioned one lattice step in opposite directions from the origin (approximating the diquark), and the third is placed from 1 to 12 lattice steps in an orthogonal direction, as shown in Fig. 2.

In this work we have used 300 quenched QCD gauge field configurations created with the $\mathcal{O}(a^2)$ -mean-field improved Luscher-Weisz plaquette plus rectangle gauge action [13] on $16^3 \times 32$ lattices with the long dimension being the x direction, making the spatial volume $16^2 \times 32$. Two hundred of these configurations were at $\beta = 4.60$ (as in our previous work) and one hundred at $\beta = 4.80$, to investigate the use of a finer lattice. These values of β give lattice spacings a of 0.123 fm and 0.0945 fm respectively.

We use lattice symmetries to improve the signal to noise ratio of our measurements. These include translational invariance (any point on the lattice can be taken as the origin), reflection in the x plane and 90° rotational symmetry about the x -axis. The advantage of this approach is that we do not have to perform any gauge fixing to find a signal in our flux distributions.

We characterise the gluon-field fluctuations in our configurations using the gauge-invariant action density $S(\vec{y}, t)$ observed at spatial coordinate \vec{y} and Euclidean time t relative to the origin of the Wilson loop. We calculate the action density using the highly-improved $\mathcal{O}(a^4)$ three-loop improved lattice field-strength tensor [12] on four-sweep APE-smearred gauge links. While the use of this highly-improved action suppresses correlations close to the quark positions, it gives good resolution of the flux-tube correlations we are interested in.

Defining the quark positions as \vec{r}_i relative to the origin of the Wilson loop, and denoting the Euclidean time extent of the loop by τ , we evaluate the following correlation functions

$$C_{3Q}(\vec{y}; \vec{r}_1, \vec{r}_2, \vec{r}_3; \tau) = \frac{\langle W_{3Q}(\vec{r}_1, \vec{r}_2, \vec{r}_3; \tau) S(\vec{y}, \tau/2) \rangle}{\langle W_{3Q}(\tau) \rangle \langle S(\vec{y}, \tau/2) \rangle}, \quad (4)$$

$$C_{Q\bar{Q}}(\vec{y}; \vec{r}_1, \vec{r}_2; \tau) = \frac{\langle W_{Q\bar{Q}}(\vec{r}_1, \vec{r}_2; \tau) S(\vec{y}, \tau/2) \rangle}{\langle W_{Q\bar{Q}}(\tau) \rangle \langle S(\vec{y}, \tau/2) \rangle}, \quad (5)$$

where $\langle \dots \rangle$ denotes averaging over configurations and lattice symmetries. These correlate the quark positions, via the Wilson loops, with the gauge-field action in a gauge invariant manner. For fixed quark positions and Euclidean time, the correlation functions are scalar fields in three dimensions. For values of \vec{y} well away from the quark positions \vec{r}_i , there are no correlations and $C \rightarrow 1$. Also the correlators are positive definite, eliminating any sign ambiguity on whether vacuum field fluctuations are enhanced or suppressed in the presence of static quarks. We find that C is generally less than 1, signaling the expulsion of vacuum fluctuations from the interior of hadrons.

In Figs. 3 and 4 we show examples of the expulsion of vacuum fluctuations and the formation of flux-tubes for our quark-diquark and quark-antiquark configurations.

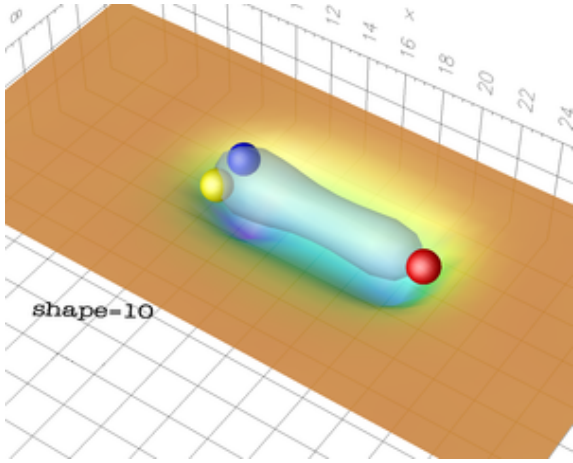


FIG. 3: Expulsion of gluon-field fluctuations from the region of static quark sources illustrated by the spheres. An iso-surface of $C(\vec{y})$ is illustrated by the translucent surface. A surface plot (or rubber sheet) describes the values of $C(\vec{y})$ for \vec{y} in the quark plane, $(y_1, y_2, 0)$.

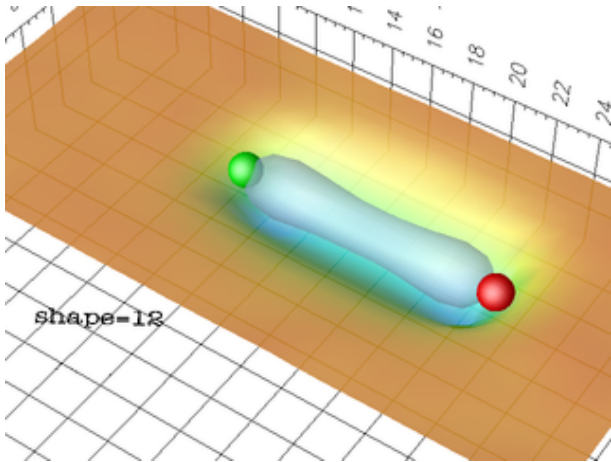


FIG. 4: Formation of quark-antiquark flux-tube. Details are as in 3

III. EFFECTIVE POTENTIALS

In this section we extract the long range portion of the potential for our quark-antiquark and quark-diquark flux-tubes. According to QCD, the effective potentials should have the same slope, so long as the APE smearing in the spatial directions has smoothed the gluon fluctuations sufficiently to isolate the ground state and the propagation of the Wilson loops in the time direction is long enough for any excited states to decay. The effective potential is obtained from the Wilson loops in the standard manner:

$$aV(\vec{r}, \tau) = \ln \left(\frac{W(\vec{r}, \tau)}{W(\vec{r}, \tau + 1)} \right). \quad (6)$$

As shown in Fig. 5 and 6, we obtain stable plateaus for the potentials as a function of τ . The statistical uncer-

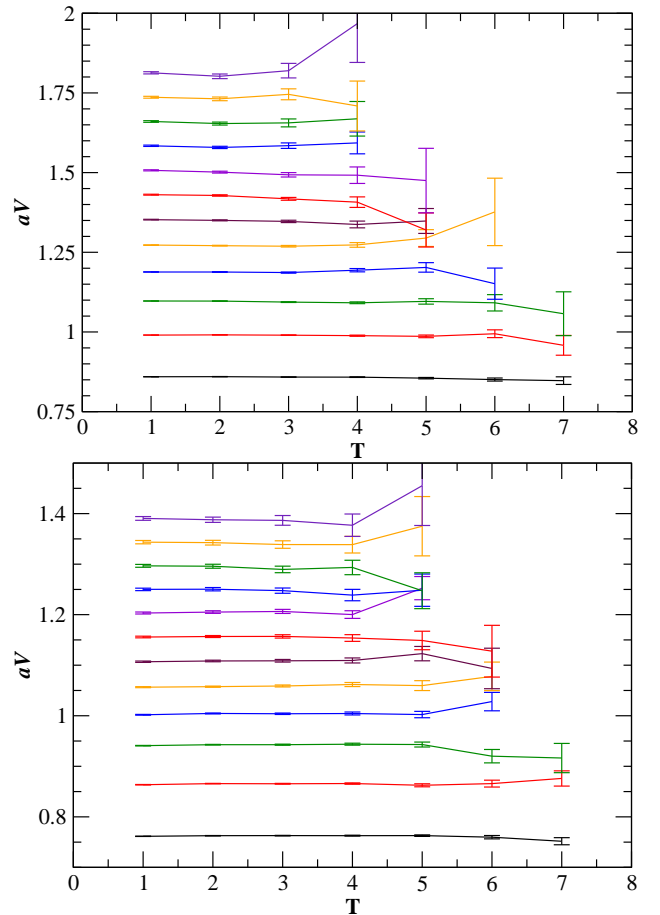


FIG. 5: Effective static quark potential for 30-sweep smeared quark-diquark sources for $\beta = 4.6$ (top) and $\beta = 4.8$ (bottom). From bottom up, the lines correspond to quark-diquark separation increasing from 1 to 12 lattice spacings.

ainties are estimated using the jackknife method [14].

The quark-antiquark potential has the well-known form

$$V_{Q\bar{Q}}(r) = V_0 - \frac{\alpha}{r} + \sigma_{Q\bar{Q}}r, \quad (7)$$

where σ is the string tension. The three quark potential is [9, 10]

$$V_{3Q}(r) = \frac{3}{2}V_0 - \frac{1}{2} \sum_{j < k} \frac{g^2 C_F}{4\pi r_{jk}} + \sigma_{3Q}L(r), \quad (8)$$

where $C_F = 4/3$ and $L(r)$ is a length linking the quarks. As shown in our earlier work [11], $L(r)$ is given by the minimum length of string that connects the three quarks, or the sum of distances from the quarks to the Fermat (or Steiner) point. QCD suggests that the two string tensions $\sigma_{Q\bar{Q}}$ and σ_{3Q} are equal. In Fig. 7 we plot the extracted effective potentials for the quark-diquark and quark-antiquark flux-tubes at each of the values of β for our gauge configurations. The plots in fermi show that the QCD prediction is confirmed at both values of β . Converting length measurements from lattice

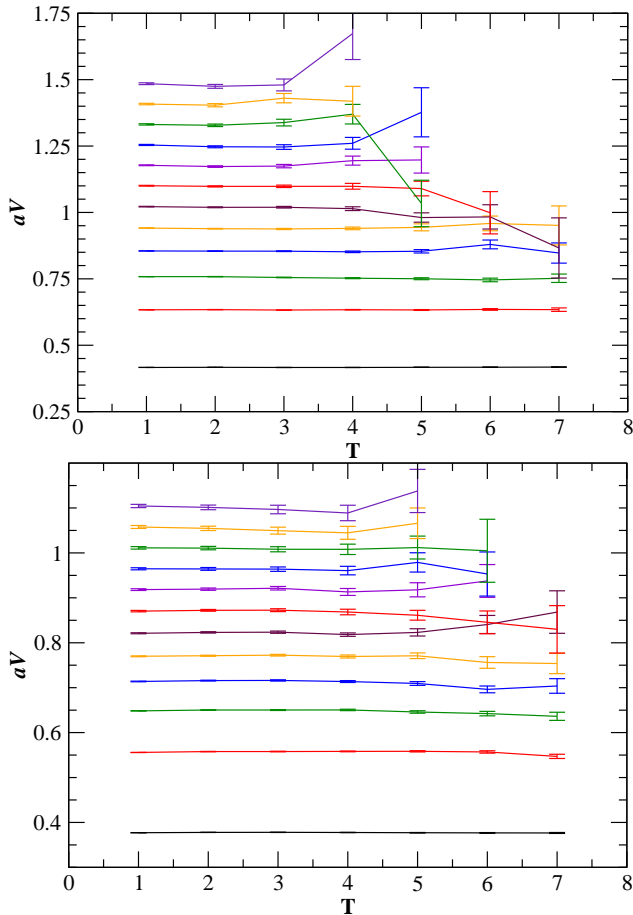


FIG. 6: Effective static quark potential for 30-sweep smeared quark-antiquark sources for $\beta = 4.6$ (top) and $\beta = 4.8$ (bottom). From bottom up, the lines correspond to quark-diquark separation increasing from 1 to 12 lattice spacings.

units to fermi we obtain the quark-diquark string tension $\sigma_{3Q} = 0.97 \pm 0.01 \text{ GeV fm}^{-1}$, which is in excellent agreement with the quark-antiquark string tension $\sigma_{Q\bar{Q}} = 0.98 \text{ GeV fm}^{-1}$, defining the lattice spacing.

IV. FLUX-TUBE PROFILES

We can gain further insight into the properties of the flux tubes by examining their profiles close to the quark. We study the values of the correlators $C_{3Q}(\vec{y})$ and $C_{Q\bar{Q}}(\vec{y})$ where $\vec{y} = (y_1, y_2, 0)$ is constrained to the plane of the color sources, and the origin is at the position of either the antiquark or the join of the T. The quark is then at the position $(\xi, 0, 0)$ where ξ varies from 1 to 12 lattice steps.

First we examine the longitudinal profiles of both quark-diquark and quark-antiquark flux-tubes along the line $(\vec{y}) = (x, 0, 0)$ in Fig. 8. As expected, the vacuum expulsion close to the diquark is stronger than in the vicinity of the antiquark. However, near the quark the two flux tubes show very similar profiles. Similar results

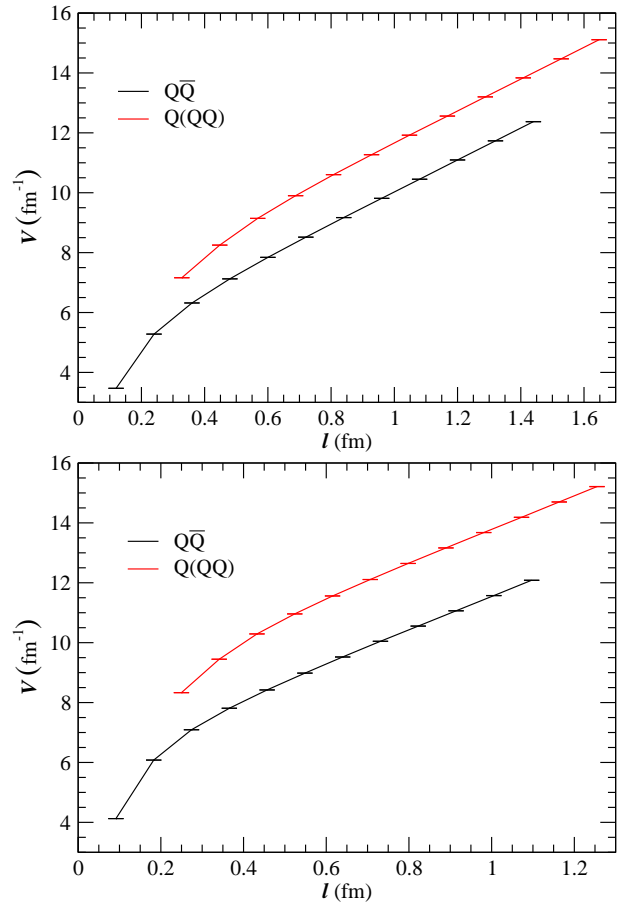


FIG. 7: Comparison of quark-antiquark and quark-diquark effective potentials for $\beta = 4.6$ (top) and $\beta = 4.8$ (bottom).

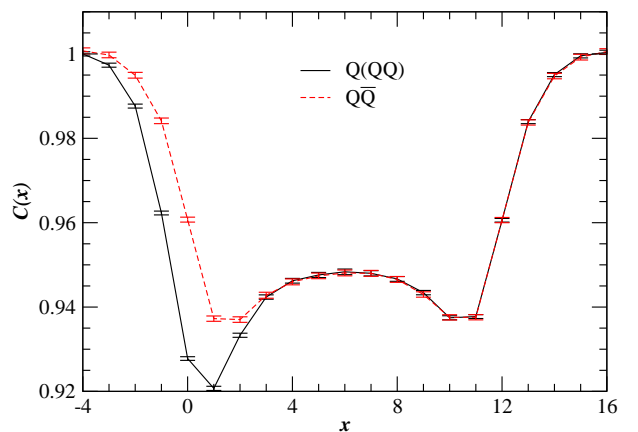


FIG. 8: Comparison of longitudinal flux tube profiles for $\beta = 4.8$ at longitudinal separation of 12 lattice units.

are seen at $\beta = 4.6$.

Next we examine the transverse profiles along a line orthogonal to the midpoint of the flux tube, *ie.* along $(\xi/2, y, 0)$ for ξ even, or along $((\xi + 1)/2, y, 0)$ for ξ odd. In Fig. 9 we show profiles of both quark-diquark and quark-antiquark flux-tubes for $\xi = 12$. We find that as

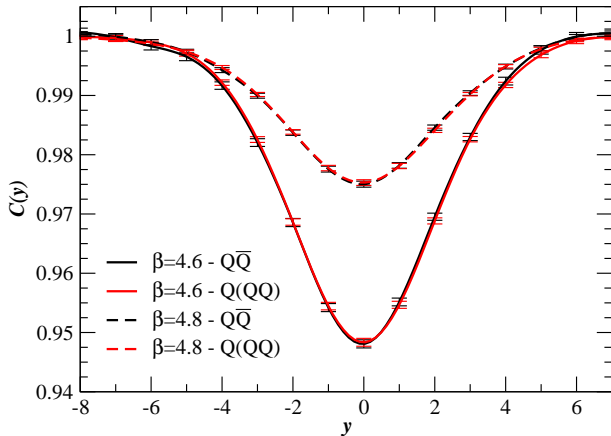


FIG. 9: Transverse profiles for quark-diquark (red lines) and quark-antiquark (black lines) flux tubes at $\beta = 4.6$ (solid lines) and $\beta = 4.8$ (dashed lines).

TABLE I: Values of the fit parameters of the function $1 - A \exp(-y^2/r^2)$ to the transverse profiles of the flux tubes. r is reported in lattice units (LU) and fm. The last column indicates the area under $C(\vec{y}) = 1$ for the fitted curve in units of relative-depth times LU.

Flux Tube	β	A	r (LU)	r (fm)	$Ar\sqrt{\pi}$
$Q\bar{Q}$	4.6	0.0511(1)	2.89(3)	0.355(3)	0.261(3)
QQQ	4.6	0.0510(1)	2.91(2)	0.358(3)	0.263(3)
$Q\bar{Q}$	4.8	0.0243(3)	3.17(4)	0.299(4)	0.136(3)
QQQ	4.8	0.0241(3)	3.21(3)	0.303(3)	0.137(3)

long as ξ is larger than one third of the total length of the quark-antiquark system, the transverse profiles are close to identical.

The transverse profile of the flux-tube is fitted well by a Gaussian function $C(y) = 1 - Ae^{-y^2/r^2}$. The fit enables us to estimate the radius (r) and area ($Ar\sqrt{\pi}$) of the flux-tube as well as its depth. The fit parameters for our flux tubes are given in Table I. Again, the fits show that for long enough flux tubes the transverse profiles of quark-diquark and quark-antiquark flux-tubes are statistically identical.

V. CONCLUSIONS

We have directly compared gluon flux-tubes for quark plus antiquark and three quark systems. In the three quark systems we kept two quarks close together (two lattice units separation), so that the system would approximate a quark-diquark string. We found that the string tension in the quark-diquark string was the same as for the quark-antiquark string. In addition we compared the vacuum expulsion in both sets of flux-tubes. We found that, in the vicinity of the quark, there was no measurable difference between the transverse profiles of the quark-diquark flux-tubes and the quark-antiquark flux-tubes. Also the longitudinal profiles of both sets of flux-tubes were very similar.

These findings confirm the expectation from QCD that a diquark has many properties in common with an antiquark. In particular the long range color interaction between a diquark and a quark is seen to be the same as that between an antiquark and a quark. This result is interesting in that it is obtained in the quenched approximation, where the color hyperfine interaction should be small. This implies that the APE smearing and propagation in Euclidean time we have performed has been sufficient for decuplet baryon states to decay. It would be interesting to repeat this work with dynamical quarks, where variation in the strength of the color hyperfine interaction could be investigated. This is potentially of great importance to phenomenological models of hadron structure.

Acknowledgments

This work has been done using the DoubleHelix computer at Massey University and supercomputing resources from the NCI National Facility and eResearch SA. The 3-D realisations have been rendered using OpenDX (<http://www.opendx.org>). The 2D plots and curve fitting have been done using Grace (<http://plasma-gate.weizmann.ac.il/Grace/>).

-
- [1] R. L. Jaffe and F. Wilczek, Phys. Rev. Lett. **91**, 232003 (2003) [arXiv:hep-ph/0307341]. R. L. Jaffe, Phys. Rept. **409**, 1 (2005) [arXiv:hep-ph/0409065].
- [2] M. Anselmino, E. Predazzi, S. Ekelin, S. Fredriksson and D. B. Lichtenberg, Rev. Mod. Phys. **65**, 1199 (1993).
- [3] M. Hess, F. Karsch, E. Laermann, and I. Wetzorke Phys. Rev. D **58**, 111502 (1998) [arXiv:hep-lat/9804023].
- [4] quarks on a large lattice. L. Lellouch, C. Rebbi and N. Shore R. Babich *et al.* JHEP **0601** 086 (2006) [arXiv:hep-lat/0509027].
- [5] K. Orginos Proc. Science LAT2005, 054 (2006) [arXiv:hep-lat/0510082].
- [6] C. Alexandrou, Ph. de Forcrand and B. Lucini Phys. Rev. Lett. **97**, 222002 (2006) [arXiv:hep-lat/0609004].
- [7] simulations. Z. Liu and T. DeGrand Proc. Science LAT2006 116 (2006) [arXiv:hep-lat/0609038].
- [8] R. Babich *et al.* Christian Hoelbling, [arXiv:hep-lat/0701023].
- [9] T. T. Takahashi, H. Matsufuru, Y. Nemoto and H. Suganuma, Phys. Rev. Lett. **86**, 18 (2001). T. T. Takahashi, H. Suganuma, Y. Nemoto and H. Matsufuru, QCD, Phys. Rev. D **65**, 114509 (2002) [arXiv:hep-lat/0204011].

- [10] C. Alexandrou, P. De Forcrand and A. Tsapalis, Phys. Rev. D **65**, 054503 (2002) [arXiv:hep-lat/0107006].
C. Alexandrou, P. de Forcrand and O. Jahn, Nucl. Phys. Proc. Suppl. **119**, 667 (2003) [arXiv:hep-lat/0209062].
- [11] F. Bissey *et al.* Nucl. Phys. Proc. Suppl. **141**, 22 (2005) [arXiv:hep-lat/0501004]; F. Bissey *et al.*, baryons,” Phys. Rev. D **76**, 114512 (2007) [arXiv:hep-lat/0606016].
- [12] S. O. Bilson-Thompson, D. B. Leinweber and A. G. Williams, Annals Phys. **304**, 1 (2003) [hep-lat/0203008].
- [13] M. Luscher and P. Weisz, Commun. Math. Phys. **97**, 59 (1985) [Erratum-ibid. **98**, 433 (1985)].
- [14] I. Montvay and G. Münster, “Quantum Fields on a Lattice” (Cambridge, 1994) 389.